

The EUMETSAT  
Network of  
Satellite  
Application  
Facilities



**O3M SAF**

Ozone and Atmospheric  
Chemistry Monitoring

## FORLI-HNO<sub>3</sub>

COMPLEMENT TO FORLI ATBD/ DESCRIPTIONS OF THE INPUTS TO FORLI-HNO<sub>3</sub> v20151001

Prepared by	Daniel Hurtmans (ULB) Catherine Wespes (ULB) Pierre-François Coheur (ULB) Rosa Astoreca (ULB)	November 16 , 2015
-------------	--	--------------------

### Reference documents

- SAF/O3M/ULB/FORLI\_ATBD
- SAF/O3M/ULB/FORLI\_SFTIC

**TABLE OF CONTENTS**

**1. INTRODUCTION .....3**

**2. INPUT PARAMETERS FOR V20151001 .....4**

2.1 IASI radiances: LIC data ..... 4

2.2 Meteorological data from the Level 2 Product Processing Facility (PPF) ..... 4

2.2.1 Temperature and humidity profiles ..... 4

2.2.2 Surface temperature..... 4

2.2.3 Cloud fraction..... 4

2.2.4 CO<sub>2</sub> profile ..... 4

2.3 Surface properties ..... 4

2.3.1 Orography..... 4

2.3.2 Emissivity..... 4

2.4 Optimal Estimation..... 5

2.4.1 *A priori* profiles and variance-covariance matrix..... 5

2.4.2 Retrieval noise..... 5

2.5 Look-up-tables..... 6

2.6 Spectroscopy..... 6

**REFERENCES.....7**

## 1. INTRODUCTION

This document is a complement to the FORLI ATBD and describes the input parameters for FORLI-HNO3 v20151001. These include the L1C measurements, meteorological data, ancillary data, input parameters for the Optimal Estimation method and the look-up tables.

## **2. INPUT PARAMETERS FOR V20151001**

### **2.1 IASI radiances: L1C data**

v20151001 uses the Level1C disseminated by EUMETCast. A subset of the spectral range, covering 860-900  $\text{cm}^{-1}$ , is used for the retrieval.

### **2.2 Meteorological data from the Level 2 Product Processing Facility (PPF)**

The IASI Level2 Product Processing Facility (IASI L2 PPF) has a modular structure, consisting of an operational processing chain, operational since 14/09/2010. It provides temperature and humidity profile information, the associated surface information and the retrieval of some trace gas species: CO, O<sub>3</sub>, CH<sub>4</sub>, N<sub>2</sub>O and CO<sub>2</sub> (August et al., 2012).

#### **2.2.1 Temperature and humidity profiles**

Profiles of temperature and humidity are from the IASI L2 PPF (August et al., 2012). The atmospheric temperatures are kept fixed whereas the water profile is used as a priori and further adjusted.

#### **2.2.2 Surface temperature**

Surface temperatures (land and sea) are from the IASI L2 PPF. Surface temperature is part of the parameters to be retrieved.

#### **2.2.3 Cloud fraction**

v20151001 uses the cloud fraction from the IASI L2 PPF. All pixels with a cloud fraction equal to or lower than 25 % are processed.

#### **2.2.4 CO<sub>2</sub> profile**

A constant vertical profile at 380 ppm is assumed for CO<sub>2</sub>.

### **2.3 Surface properties**

#### **2.3.1 Orography**

Orography is from the GTOPO30 global digital elevation model and is integrated in the entire IASI FOV ([http://eros.usgs.gov/#/Find\\_Data/Products\\_and\\_Data\\_Available/gtopo30\\_info](http://eros.usgs.gov/#/Find_Data/Products_and_Data_Available/gtopo30_info)).

#### **2.3.2 Emissivity**

A wavenumber-dependent surface emissivity above continental surfaces is used while for ocean a single standard emissivity is considered. For continental surfaces it relies on the climatology of Zhou et al. (2011). In cases of missing values in the Zhou et al. climatology, the MODIS climatology of Wan (2008) is used. It is available on a finer  $0.05^\circ \times 0.05^\circ$  grid but is restricted to only 12 channels in the IASI spectral range. In order to deal with this, the spectrally resolved mean emissivity of the Zhou climatology is scaled to match as closely as possible the values in these 12 channels and it is this resulting emissivity that is considered. Finally when there is no correspondence between the IASI FOV and either climatologies, then the mean emissivity of the Zhou climatology is used.

## 2.4 Optimal Estimation

### 2.4.1 *A priori* profiles and variance-covariance matrix

The *a priori* information was inferred from a combination of model calculations for the tropospheric component and from satellite limb measurements for the upper troposphere up to the stratosphere. More specifically, daily profiles from the LMDz-INCA chemistry-transport model (Hauglustaine et al., 2004), generated on a  $3.75^\circ \times 2.50^\circ$  longitude–latitude grid over one year have been selected, from the ground up to 15.6 km. Additionally all measured profiles from 6 to 60 km from the Atmospheric Chemistry Experiment (ACE-FTS) (Bernath et al., 2005; Boone et al., 2005) for over two years (2004–2006) are included in the ensemble. From there a full variance–covariance matrix and a mean (*a priori*) profile  $\mathbf{x}_a$  are calculated (Fig.3).  $\mathbf{x}_a$  is pretty constant in volume mixing ratio throughout the troposphere. In terms of molecular densities, this translates to values around  $5 \times 10^9$  molecules/cm<sup>3</sup> in the boundary layer, slowly decreasing with altitude up to 8 km, then increasing to a maximum up to  $1.2 \times 10^{10}$  at 18 km; the tropospheric layer 0–10 km makes up 21% of the total column (see also Wespes et al. 2009). The variability around the *a priori* is large, especially in the boundary layer, where it reaches 170%. Furthermore, the tropospheric and stratospheric layers are weakly correlated, as expected, while within these two layers the correlation lengths are significant.

### 2.4.2 Retrieval noise

The value of the noise is wavenumber dependent in the spectral range used for the retrieval, varying around  $2 \times 10^{-8}$  W/(cm<sup>2</sup> cm<sup>-1</sup> sr).

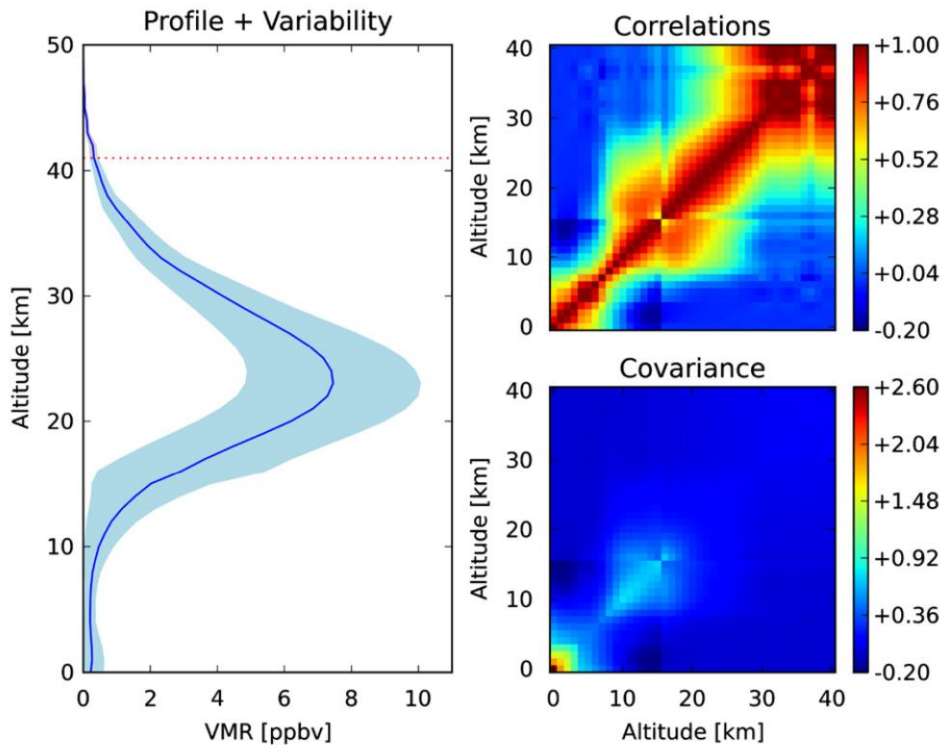


**Figure 1.** Left:  $\mathbf{x}_a$  (ppmv, blue line) and associated variance (shaded blue) for the FORLI-HNO<sub>3</sub>. The dashed red line indicates the top altitude of the last retrieved layer. Right: correlations and  $\mathbf{S}_a$  variance–covariance matrices in multiplication factor (from Hurtmans et al. 2012)

## 2.5 Look-up-tables

Tabulated absorption cross-sections at various pressures and temperatures are used to speed up the radiative transfer calculation. The spectral range for the LUTs used in v20151001 is 810-960 cm<sup>-1</sup> and the spectral oversampling is 25. The absorption cross-sections are computed on a logarithmic grid for pressure from  $4.5 \times 10^{-5}$  to 1 atm with a grid step of 0.2 for the logarithm of pressure, and on a linear grid for temperature (162.8–322.6 K with a grid step of 5K). Relative humidity is also introduced in the LUT, varying linearly between 0 and 100%, by steps of 10%.

## 2.6 Spectroscopy

Line integrated absorption cross section, air broadening, self-broadening, line shifting and absorption cross section data are taken from the widely used HITRAN spectroscopic database online version (hitran.org). Continuum formulations are taken from MT-CKD (Clough et al., 2005).

## REFERENCES

- August, T., Klaes, D., Schlüssel, P., Hultberg, T., Crapeau, M., Arriaga, A., O'Carroll, A., Coppens, D., Munro, R. & Calbet, X. IASI on Metop-A: Operational Level 2 retrievals after five years in orbit. *J. Quant. Spectrosc. Radiat. Transfer*, 113, 1340-1371, 2012.
- Bernath P, McElroy C, Abrams M, Boone C, Butler M, Camy-Peyret C, et al. Atmospheric Chemistry Experiment (ACE): mission overview. *Geophys Res Lett* ;32(15). doi:10.1029/2005GL022386, 2005.
- Boone C, Nassar R, Walker K, Rochon Y, McLeod S, Rinsland C, et al. Retrievals for the Atmospheric Chemistry Experiment Fourier- transform spectrometer. *Appl Opt*;44(33):7218–31, doi:10.1364/AO.44.007218, 2005.
- Clough, S, Shephard, M, Mlawer, E, Delamere, J, Iacono, M, Cady-Pereira K, Boukabara, S., Brown, P.D., Atmospheric Radiative Transfer Modeling: a Summary of the AER Codes, *J. Quant. Spectrosc. Radiat. Transfer*, 91, 233-244, 2005
- Hauglustaine D, Hourdin F, Jourdain L, Filiberti M, Walters S, Lamarque J, et al. Interactive chemistry in the Laboratoire de Meteorologie Dynamique general circulation model: description and background tropospheric chemistry evaluation. *J Geophys Res (Atmos)*;109(D4). doi:10.1029/2003JD003957, 2004.
- Hurtmans, D.; Coheur, P.; Wespes, C.; Clarisse, L.; Scharf, O.; Clerbaux, C.; Hadji-Lazaro, J.; George, M. & Turquety, S. FORLI radiative transfer and retrieval code for IASI. *J. Quant. Spectrosc. Radiat. Transfer*, 113, 1391-1408, 2012.
- Wan Z. New refinements and validation of the MODIS Land-Surface Temperature/Emissivity products. *Remote Sens. Environ.*, 112(1):59-74, 2008.
- Wespes C, Hurtmans D, Clerbaux C, Santee ML, Martin RV, Coheur PF. Global distributions of nitric acid from IASI/MetOp measurements. *Atmos Chem Phys*;9(20):7949–62, 2009.
- Zhou, D. K.; Larar, A. M.; Liu, X.; Smith, W. L.; Strow, L. L.; Yang, P.; Schlüssel, P. & Calbet, X. Global Land Surface Emissivity Retrieved From Satellite Ultraspectral IR Measurements. *IEEE Trans. Geosci. Remote Sens.*, 49(4):1277-1290, 2011.



REFERENCE: SAF/O3M/ULB/FORLIHNO3\_CATBD

ISSUE: 1.0

DATE: 16 November, 2015

PAGES: Page 8 of 8

---